Stacked Generalization for Enhanced Embedded Element Pattern Prediction in Non-Uniform Arrays

Nehir Berk Onat, Ignacio Roldan, Francesco Fioranelli, Alexander Yarovoy, and Yanki Aslan

Abstract – A novel stacked generalization method is proposed to enhance the prediction of embedded element patterns (EEPs) under mutual coupling effects. The proposed technique employs a meta model with two base models as follows: a two-stage neural network (NN) for direct EEP prediction from full-wave generated data and a fully connected NN to estimate infinitesimal dipole modeling coefficients, approximating full-wave EEPs via constrained IDM. The meta model determines optimal weighting matrices for each base model to leverage their localized strengths. This approach addresses the challenge of maintaining sufficient pattern prediction accuracy with relatively small datasets. The effectiveness of the approach is demonstrated using nonuniformly spaced five-element pin-fed patch antenna arrays.

1. Introduction

Nonuniformly spaced (aperiodic) arrays have emerged as a promising solution for achieving superior performance in phased array antenna systems for various communication and sensing systems [1, 2]. These arrays offer significantly lower side-lobe levels during wide-angle scanning while maintaining comparable or higher gain than their uniformly spaced counterparts [3, 4]. However, the high potential of aperiodic arrays relies on the accurate modeling and prediction of mutual coupling (MC) effects, a complex challenge that has long impeded the efficient and reliable synthesis of such systems [5].

In aperiodic arrays, MC effects are particularly significant because of the nonuniform spacing between elements, which makes the interactions between antennas more unpredictable compared with uniform arrays during the synthesis process. Neglecting or oversimplifying the MC effects, as often done using isolated-element or infinite-array assumptions, can lead to unreliable designs with degraded radiation performance in practice. Although full-wave simulations can provide accurate insight into MC for specific aperiodic configurations [6], the computational demands of such methods make them impractical for the iterative and requirement-specific optimizations required in the design of aperiodic arrays.

In recent years, machine learning (ML) and, particularly, neural networks (NNs) have gained attention as powerful tools for addressing complex electromagnetic challenges with remarkable efficiency [7, 8]. Recently, ML has been applied to various antenna design and array synthesis problems, primarily focusing on element geometry optimization [9] and excitation control to maximize wireless power transfer [10] or minimize side lobe levels [11, 12]. On the other hand, NNs are particularly well-suited for approximating the embedded element patterns (EEPs) of antennas, as proposed in [13, 14], capturing the non-linear mutual coupling effects on the radiation, which is necessary for accurate beamforming. However, as discussed in our URSI-RASC 2024 paper [15], the performance of NNs is influenced by the size and distribution of the dataset; smaller datasets tend to increase error variability, while MC effects can decrease reliability.

An ensemble prediction framework was proposed in [16] to achieve accurate and fast EEP prediction under varying MC effects with a reduced training dataset. This was achieved by manually applying a weighted sum to the prediction results from the base models, where the weighting factor, β, is optimally chosen based on the performance of the base models on the validation set. However, such manual strategies fail to exploit the localized advantages of each method (for instance, one network may provide superior estimation of the main lobe, while the other may perform better in estimating side-lobe levels).

In this paper, we propose a new stacked generalization model where the meta model via the custom Hadamard layer:

- determines optimal weighting matrices for each base model to exploit their localized strengths,
- eliminates the averaging error caused by the manual computation over the validation set,
- enables multiple base model integration to enhance the prediction performance.

The rest of the paper is organized as follows. Section 2 presents the antenna under test (AUT) and problem formulation. The existing methodologies and proposed ensemble learning are explained in Sections 3

Manuscript received 15 December 2024.

Nehir Berk Onat, Ignacio Roldan, Francesco Fioranelli, Alexander Yarovoy, and Yanki Aslan are with Microelectronics Department, Delft University of Technology, Mekelweg 4, 2628 Delft, The Netherlands; e-mail: n.b.onat@tudelft.nl, i.roldanmontero@tudelft.nl, f.fioranelli@tudelft.nl, a.yarovoy@tudelft.nl, y.aslan@tudelft.nl.

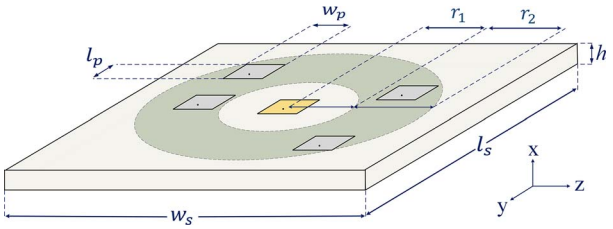

Figure 1. Five-element aperiodic array topology where the AUT, highlighted with the yellow color, is located at the center, $(y_o, z_o) = (0, 0)$, and the neighboring elements are randomly positioned in the defined green region: $r_1^2 \le (y_i^2 + z_i^2) \le (r_1 + r_2)^2$, where (y_i, z_i) is the location of the i-th neighbor element in λ [16].

and 4, respectively. The simulation results are discussed in Section 5, and Section 6 concludes the paper.

2. Problem Formulation

To ensure consistency with the methodologies in [15] and [16], this study employs the same five-element, irregularly spaced, pin-fed patch array topology operating at the same center frequency, 2.85 GHz, as depicted in Figure 1. The AUT is positioned at the center of the array's aperture. At the same time, the neighboring elements are confined to a defined region (highlighted in green in Figure 1) bounded by an inner and outer circle. The inner circle has a radius corresponding to the minimum element spacing, $r_1 = \lambda/2$, r_2 is set equal to r_1. This configuration maintains the elements close to each other, allowing for the observation of the MC effects on the EEP for varied array topologies.

The pattern error is computed for the region $20^\circ \le \theta \le 160^\circ$ and $-70^\circ \le \phi \le 70^\circ$ describing the angular region of interest for common array applications, where θ and ϕ follow the standard spherical coordinate system. To quantify the error between the predicted and full-wave generated EEP, the mean squared error (MSE) is used [16]:

$$\varepsilon_p = 10\lg\left(\frac{1}{N_s^2}\sum_{i,j=1}^{N_s}\left(\,|\,EEP_{\text{fw}}(\theta_i,\phi_j)\,|\,-\,|\,EEP'_p(\theta_i,\phi_j)\,|\,\right)^2\right) \tag{1}$$

where N_s denotes the number of samples for the spherical angles θ and ϕ, EEP_{fw} is the full-wave generated far-field electric field radiation pattern of the corresponding element, and EEP'_p and ε_p are the predicted EEP of the corresponding element and its MSE. The subscript, p specifies the methodology used.

For the ML-assisted prediction of EEPs, the training data can be generated using full-wave simulations with randomized array layouts around an element under test. The power pattern of the element generated for the dataset is a function of the spherical angles θ and ϕ (e.g., each having 180 samples), resulting in a 180×180 matrix. A straightforward prediction method is a direct EEP estimation using a neural network on this dataset. An alternative method is to modify the base model and estimate the EEP under the new base. Infinitesimal dipole modeling (IDM) is atechnique that can serve as a basis [17, 18] through ID coefficients, which are used in EEP prediction via the array factor relation.

In the IDM approach, the array surface is replaced by an equivalent array of infinitesimal electric (*e*-) and magnetic (*m*-) dipoles, with excitation coefficients derived by inverting a Vandermonde-type matrix, adjusted with Gaussian noise for stability. While a dense array of *e*- and *m*-dipoles offers higher accuracy, the high condition number of the matrix makes the coefficients sensitive to errors, particularly those introduced by NNs. Previous work [19] identified an optimal tradeoff between condition number and pattern approximation error by using only *m*-dipoles oriented along the radiating edges (*z*-axis) of a patch arranged in a sunflower layout. For a maximum array radius of λ, 81 dipoles were found to be optimal where it was used to enhance array prediction performance in [16].

3. Existing EEP Prediction Methodologies

This section summarizes the two previously proposed methods used for estimating the absolute EEPs, as well as the manual ensemble method combining both [16].

3.1 Direct Estimation

The input to the proposed network $P \in \mathbb{R}^{4\times 2}$ represents the positions in polar coordinates of the antenna elements, and they are processed through a one-dimensional convolutional layer with 16 kernels to encode spatial relationships. This is followed by seven fully connected layers, incrementally increasing the number of neurons to 1296, determined through heuristic tuning. The output is reshaped into a 36×36 matrix resembling a low-resolution EEP, which is then upscaled to 180×180 using an ESPCN architecture. This involves two convolutional layers (32 filters, 36×36 kernel size) and a sub-pixel convolutional layer (25 filters) for upscaling. The model contains 2 million parameters, making it relatively lightweight, and achieves estimation speeds significantly faster than full-wave simulations. A critical component of the design is the use of the Structural Similarity Index as a loss function during training. The Structural Similarity Index enforces structural relationships between matrix elements, which are crucial for EEP accuracy, outperforming traditional loss functions, such as MSE or MAE, which treat matrix cells independently.

3.2 IDM-Based Estimation

The second approach estimates 81 z-oriented m-type ID complex excitation coefficients for the given element positions, reducing the estimation space from 32,400 to 81 coefficients. The architecture includes a one-dimensional convolutional layer with 16 kernels for

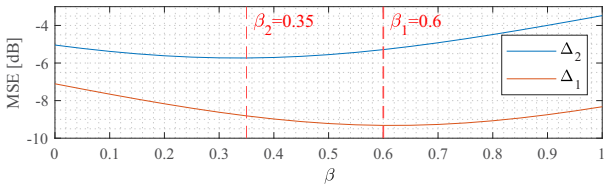

Figure 2. Analysis of the weighting value, β, for the ensemble prediction where Δ_1 and Δ_2 represent the datasets comprising 3500 and 1500 data, respectively. The MSE of each point is calculated over the validation set, where $\beta_1 = 0.6$ and $\beta_2 = 0.35$ provide the minimum error for the datasets Δ_1 and Δ_2, respectively [16].

spatial encoding, followed by seven fully connected layers to match the depth of the previous network for consistent comparisons. The final output is an 81×2 vector representing the real and imaginary parts of the coefficients. The network is trained using the ADAM optimizer with default hyperparameters ($\eta = 0.001$, $\beta_1 = 0.9$, $\beta_2 = 0.999$, $\varepsilon =$ 1e-7) and the MSE loss function to minimize the error between the predicted and true ID coefficients. Once the coefficients are estimated, the EEP is computed using the previously described IDM technique.

3.3 Empirical Ensemble Prediction

The method presented in [16] employed two distinct networks, base models, to estimate EEPs independently (explained in the previous section), subsequently combining them to produce a more accurate EEP by leveraging the strengths of each network. The original methodology achieved this combination through a weighted average, with the weighting coefficient β determined manually over the validation set and must be recalculated whenever the dataset size or type changes.

In [16, fig 2], the change of the β depending on the dataset size is illustrated. In addition to manually determining β, a single coefficient cannot achieve consistent performance across various datasets due to differences in the prediction performance of the base models.

4. Proposed Technique: Stacked Generalization

The proposed method replaces the simple weighted average discussed in Section 3.3 with a newly trained, single-layer network to enhance prediction performance. This network uses a custom layer designed specifically for this application, which computes the Hadamard product of the preliminary EEPs and adds them as follows:

$$EEP_{\mathrm{ENS}} = EEP_{\mathrm{NN}} \odot A + EEP_{\mathrm{IDM-NN}} \odot B \tag{2}$$

where $\odot$ is the Hadamard product and $A \in \mathbb{R}^{140\times140}$ and $B \in \mathbb{R}^{140\times140}$ are the weights. EEP_{ENS}, EEP_{NN}, and $EEP_{\mathrm{IDM-NN}}$ denote the predicted EEPs by the meta, NN-direct, and IDM-NN models, respectively, given in Figure 3 . The network aims to find the optimal matrices A and B to maximize the prediction accuracy. With this, it is possible to have different averages for different EEP regions, exploiting each method's advantages.

Figure 3 shows the block diagram of the full approach. For this work, each network has been trained independently. The first two networks were trained as described in [16]. The single-layer ensemble has been trained using the Adam optimizer and MSE as the loss function. Either 1500 (dataset Δ_1) or 3500 (dataset Δ_2) EEPs have been used for training, 200 for validation, and 50 for tests. All the results presented in the next section are computed in the test set, with data completely unseen for the network.

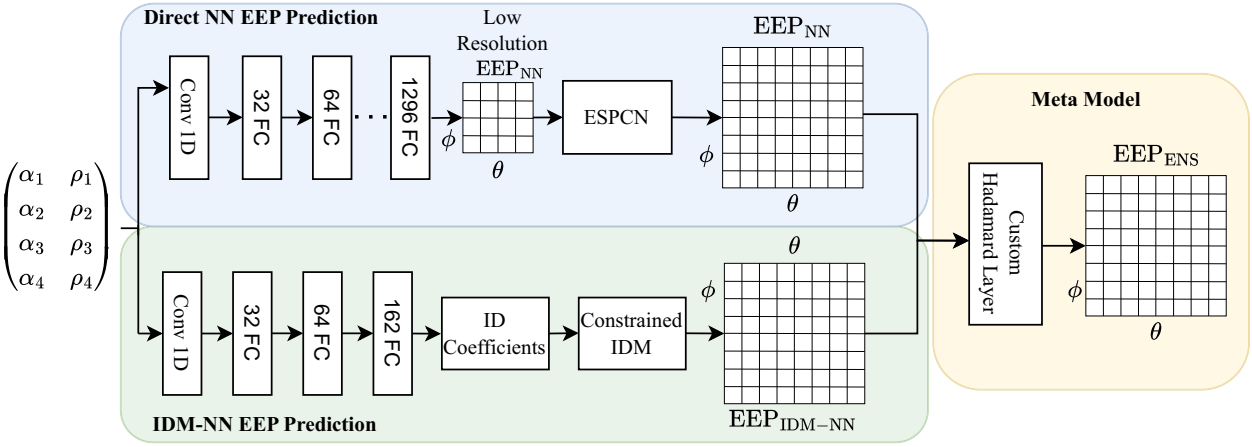

Figure 3. The block diagram of the proposed approach. The lower path (green) comprises an NN for estimating the ID-complex coefficients, which is used to reconstruct the EEP via constrained IDM. In the upper path (blue), a two-stage network and the ESPCN architecture are used to predict the EEP directly. The proposed meta model (yellow), the custom Hadamard layer, enhances the prediction performance from preliminary predictions of the base models.

Table 1. The average MSE results and comparison of the models trained with Δ_1 and Δ_2 with the additional results of two example cases of these models trained with the dataset Δ_1

	Dataset		Cases with Δ_1	
Error (MSE)	Δ_1	Δ_2	Case 1	Case 2
ε_{IEP} (dB)	−10.56	−10.56	−11.61	−12.29
ε_{NN} [dB] [13]	−16.10	−18.85	−15.66	−24.63
$\varepsilon_{\text{IDM-NN}}$ (dB) [16]	−16.54	−19.60	−18.50	−18.34
ε_{ENS} (dB) [this work]	−17.73	−21.02	−19.67	−24.64

5. Simulation Results

To demonstrate the superior performance of the proposed technique, the ensemble predicted EEP via stacked generalization (EEP_{ENS}) is compared with the full-wave simulated isolated element pattern, and the two most relevant state-of-the-art benchmark methodologies, NN-direct predicted EEP (EEP_{NN}) [13], and IDM-NN predicted EEP ($\text{EEP}_{\text{IDM-NN}}$) [16]. Table 1 shows the comparison of the results.

Although the meta model learns how to weigh the predictions of each base model to enhance the final prediction, it improves the average MSE (ε_{ENS}) over the test set, achieving −17.73 dB and −21.02 dB on average with the datasets Δ_1 and Δ_2, respectively. Although the proposed base models perform well with larger datasets, their performance begins to fluctuate with the smaller dataset, reducing the reliability of the predictions, which is partly reflected in the average MSE shown in Table 1. To illustrate this, two array topologies (Cases 1 and 2) from the test set are chosen where the models are trained with the smaller dataset, Δ_1.

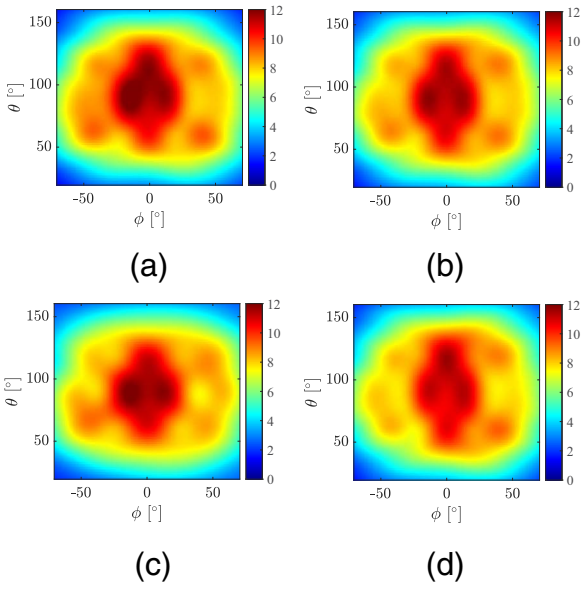

Figure 4. EEP (in dB) comparison in case topology 2 with $(y_i, z_i) = \{(-0.60, -0.10), (0.25, -0.50), (0.20, 0.60), (0.70, -0)\}\lambda$, and AUT is located at the origin. (a) Full-wave generated EEP, (b) EEP_{ENS} [this work], (c) $\text{EEP}_{\text{IDM-NN}}$ [16], and (d) EEP_{NN} [13].

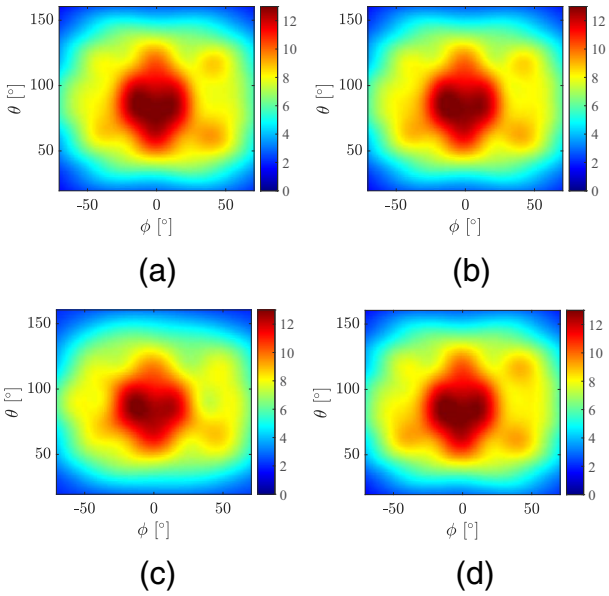

Figure 5. EEP (in dB) comparison in case topology 2 with $(y_i, z_i) = \{(0.30, 0.60), (-0.50, 0.60), (-0.20, -0.60), (-0.65, -0.20)\}\lambda$ and AUT is located at the origin. (a) Full-wave generated EEP, (b) EEP_{ENS} [this work], (c) $\text{EEP}_{\text{IDM-NN}}$ [16], and (d) EEP_{NN} [13].

In case topology 1, while the IDM-NN model achieves an MSE ($\varepsilon_{\text{IDM-NN}}$) of −18.50 dB, the error of the NN-direct model (ε_{NN}) remains at −15.66 dB above the average MSE. The difference in error can also be observed on the EEPs where the NN-direct fails to predict the high-gain region accurately, as illustrated in Figure 4. On the other hand, the proposed meta model improves the prediction performance and reduces the MSE to −19.67 dB, which is below the average MSE. As Figure 4 shows, the final predicted EEP comprises the localized accuracies of the preliminary predictions.

In some rare cases, one method may significantly outperform the other. In such instances, the meta model must intelligently combine the predictions, giving more weight to the base model that provides the more accurate result. Figure 5 presents the case topology 2, where the NN-direct model delivers one of the best predictions, achieving an MSE of −24.63 dB, while the IDM-NN model remains above −18.5 dB. As expected, the proposed meta model accurately generates the final prediction by weighing the NN-direct model's prediction, resulting in an MSE of −24.64 dB, as shown in Figure 5.

6. Conclusion

This paper presents a novel stacked generalization method designed to improve the prediction accuracy of EEPs under the MC effects. The approach combines the following two base models: a two-stage NN for direct EEP prediction using full-wave generated data and a fully connected NN for estimating IDM coefficients, which approximate full-wave EEPs through

constrained IDM. A key innovation of the proposed method lies in its meta-model, which determines optimal weighting matrices for each base model to exploit their localized strengths. This eliminates averaging errors associated with manual computations. Furthermore, the framework supports the integration of multiple base models, enhancing overall prediction performance. The effectiveness of the proposed method is validated on nonuniformly spaced five-element pin-fed patch antenna arrays, demonstrating its capability to deliver accurate and efficient EEP predictions. This work establishes a foundation for developing more robust prediction methodologies for complex antenna systems, especially in scenarios where dataset size and accuracy are critical constraints.

7. References

1. X. Ge, R. Zi, H. Zhai, J. Zhang, and M. Jo, "Multi-User Massive MIMO Communication Systems Based on Irregular Antenna Arrays," *IEEE Transactions on Wireless Communications*, **15**, 8, 2016, pp. 5287-5301.
2. C. Bencivenni, M. V. Ivashina, R. Maaskant, and J. Wettergren, "Synthesis of Maximally Sparse Arrays Using Compressive Sensing and Full-Wave Analysis for Global Earth Coverage Applications," *IEEE Transactions Antennas Propagation*, **64**, 11, 2016, pp. 4872-4877.
3. O. M. Bucci, M. D'Urso, T. Isernia, P. Angeletti, and G. Toso, "Deterministic Synthesis of Uniform Amplitude Sparse Arrays via New Density Taper Techniques," *IEEE Transactions Antennas Propagation*, **58**, 6, 2010, pp. 1949-1958.
4. Y. Aslan, J. Puskely, A. Roederer, and A. Yarovoy, "Multiple Beam Synthesis of Passively Cooled 5G Planar Arrays Using Convex Optimization," *IEEE Transactions Antennas Propagation*, **68**, 5, 2020, pp. 3557-3566.
5. H. Singh and R. Jha, "Mutual Coupling in Phased Arrays: A Review," *International Journal of Antennas Propagation*, 2013, 5, **2013**. doi: 10.1155/2013/348123.
6. C. Bencivenni, M. V. Ivashina, R. Maaskant, and J. Wettergren, "Design of Maximally Sparse Antenna Arrays in the Presence of Mutual Coupling," *IEEE Antennas Wireless Propagation Letters*, **14**, 2015, pp. 159-162.
7. A. Massa, D. Marcantonio, X. Chen, Mo. Li, and M. Salucci, "DNNs as Applied to Electromagnetics, Antennas, and Propagation—A Review," *IEEE Antennas Wireless Propagation Letters*, **18**. 11, 2019, pp. 2225-2229.
8. C. Cui, W. T. Li, X. T. Ye, Y. Q. Hei, P. Rocca, et al. "Synthesis of Mask-Constrained Pattern-Reconfigurable Nonuniformly Spaced Linear Arrays Using Artificial Neural Networks," *IEEE Transactions on Antennas and Propagation,* **70**, 6, 2022, pp. 4355-4368.
9. Q. Wu, W. Chen, C. Yu, H. Wang, and W. Hong, "Machine-Learning-Assisted Optimization for Antenna Geometry Design," *IEEE Transactions on Antennas and Propagation,* **72**, 3, 2024, pp. 2083-2095.
10. D, Xiao, L. Tian, L. Xu, H. Zhang, and X. Wang, "Fast Beam-Pointing Control Algorithms Based on Deep Learning Models for Moving Target in MWPT," *IEEE Transactions on Antennas and Propagation,* **72**, 5, 2024, pp. 4541-4548.
11. A. Arce, F. Arce, E. Stevens-Navarro, U. Pineda-Rico, M. Cardena-Juarez, et al. "Recurrent Deep Learning for Beam Pattern Synthesis in Optimized Antenna Arrays," *Applied Sciences,* **15**, 1, 2024, p. 204.
12. S. A. Hamza and M. G. Amin. "Sparse Array Design for Optimum Beamforming Using Deep Learning," *IEEE Transactions on Aerospace and Electronic Systems*, **60**, 1, 2024, pp. 133-144.
13. N. B. Onat, I. Roldan, F. Fioranelli, A. Yarovoy, and Y. Aslan, "Efficient Embedded Element Pattern Prediction via Machine Learning: A Case Study with Planar Non-Uniform Sub-Arrays," presented in the 2023 17th European Conference on Antennas and Propagation (EuCAP), Florence, Italy, March 26–31, 2023.
14. Y. Jiang, S. S. A. Yuan, and W. E. I. Sha, "A Novel Mutual Coupling ANN Model for MIMO Antennas With Physical Preprocessing," *IEEE Antennas and Wireless Propagation Letters*, **23**,12, 2024, pp. 4523-4527. doi: 10.1109/LAWP.2024.3454336.
15. N. B. Onat, I. Roldan, F. Fioranelli, A. Yarovoy, and Y. Aslan, "Dataset Dependency of Data-Driven ML Techniques in Pattern Prediction Under Mutual Coupling," presented in the 4th URSI AT-RASC, Gran Canaria, Spain, May 19–24, 2024.
16. N. B. Onat, I. Roldan, F. Fioranelli, A. Yarovoy, and Y. Aslan, "Constrained Infinitesimal Dipole Modeling-Assisted Ensemble Prediction of Embedded Element Patterns via Machine Learning," *IEEE Transactions on Antennas and Propagation*, **72**, 9, 2024, pp. 7353-7358.
17. M. Serhir, P. Besnier, M. Drissi, "An accurate equivalent behavioral model of antenna radiation using a mode-matching technique based on spherical near field measurements," *IEEE Transactions on Antennas and Propagation*, **56**, 1, 2008, pp. 48-57.
18. M. Serhir, P. Besnier, N. Ribiere-Tharaud, and M. Drissi, "The Use of Infinitesimal Dipoles and the Spherical Wave Expansion for Planar Antennas Modeling," presented in the Proceedings of the Fourth European Conference on Antennas and Propagation, Barcelona, Spain, April 12–16, 2010.
19. N. B. Onat, A. Yarovoy, and Y. Aslan, "Sunflower Array of Infinitesimal Dipoles for Constrained Antenna Modeling," presented in the 2024 18th European Conference on Antennas and Propagation (EuCAP), March 17–22, 2024.